Received: 28 April 2022 | Accepted: 24 May 2023

DOI: 10.1111/mec.17040

ORIGINAL ARTICLE

MOLECULAR ECOLOGY WILEY

Multispecies coinfections and presence of antibiotics shape resistance and fitness costs in a pathogenic bacterium

Roghaieh Ashrafi[1] | Matthieu Bruneaux[1] | Lotta-Riina Sundberg[1,2] | Ville Hoikkala[1,2] | Anssi Karvonen[1]

[1]Department of Biological and Environmental Science, University of Jyväskylä, Jyväskylä, Finland

[2]Nanoscience Center, University of Jyväskylä, Jyväskylä, Finland

Correspondence
Roghaieh Ashrafi, Department of Biological and Environmental Science, University of Jyväskylä, P.O. Box 35, 40014 Jyväskylä, Finland.
Email: roghaieh.ashrafi@jyu.fi

Funding information
Academy of Finland, Grant/Award Number: 314939 and 310632; OLVI-Säätiö, Grant/Award Number: 201620393

Handling Editor: Kin-Ming (Clement) Tsui

Abstract

Increasing antimicrobial resistance (AMR) poses a challenge for treatment of bacterial diseases. In real life, bacterial infections are typically embedded within complex multispecies communities and influenced by the environment, which can shape costs and benefits of AMR. However, knowledge of such interactions and their implications for AMR in vivo is limited. To address this knowledge gap, we investigated fitness-related traits of a pathogenic bacterium (*Flavobacterium columnare*) in its fish host, capturing the effects of bacterial antibiotic resistance, coinfections between bacterial strains and metazoan parasites (fluke *Diplostomum pseudospathaceum*) and antibiotic exposure. We quantified real-time replication and virulence of sensitive and resistant bacteria and demonstrate that both bacteria can benefit from coinfection in terms of persistence and replication, depending on the coinfecting partner and antibiotic presence. We also show that antibiotics can benefit resistant bacteria by increasing bacterial replication under coinfection with flukes. These results emphasize the importance of diverse, inter-kingdom coinfection interactions and antibiotic exposure in shaping costs and benefits of AMR, supporting their role as significant contributors to spread and long-term persistence of resistance.

KEYWORDS
antibiotic resistance, coinfection, multispecies interactions, virulence

1 | INTRODUCTION

Global overuse of antibiotics has selected for the evolution and spread of antibiotic resistance in many bacterial species, posing a serious threat to human health and food production (World Health Organization, 2018). Resistance, evolving either by chromosomal mutation or via genetic exchange, can be a fitness benefit for bacteria in presence of antibiotics, but costly when antibiotics are absent (Alekshun & Levy, 2007; Andersson & Hughes, 2010; Melnyk et al., 2015). Costs, expressed in terms of reduced growth rate, competitive ability or virulence (Andersson & Hughes, 2010), can have important epidemiological and evolutionary consequences as antibiotic-sensitive strains may outcompete resistant ones in the absence of antibiotics (Hall, 2004; Melnyk et al., 2015). However, the presence of antibiotics can favour resistant strains by reducing or eliminating sensitive competitors, allowing persistence of the resistant strains (de Roode et al., 2004; Wargo et al., 2007). As the antibiotic resistance problem continues to worsen, empirical evidence on the costs and benefits of antibiotic resistance in naturally realistic infection scenarios is needed.

Pathogens and parasites are rarely encountered in single-species populations, but they are typically embedded within complex multispecies communities that include a range of intraspecific and interspecific interactions across different pathogen/parasite genera and phyla, even kingdoms (Bottery, Matthews, et al., 2021; Bottery, Pitchford, et al., 2021; Johnson et al., 2015; Pedersen & Fenton, 2019; Rowan-Nash et al., 2019). Such interactions can have important implications not only for virulence and transmission success but also for disease progression and treatment (Alizon et al., 2013; Bottery, Matthews, et al., 2021; de Roode et al., 2005; Hiltunen et al., 2017; Read & Taylor, 2001; Seppälä et al., 2012). There is growing recognition that intraspecific and interspecific interactions can also alter evolutionary dynamics of antibiotic resistant strains and influence susceptibility of bacteria to antibiotics (Birger et al., 2015; Bottery, Matthews, et al., 2021; Bottery, Pitchford, et al., 2021; Briaud et al., 2019; Davies et al., 2019; Estrela & Brown, 2018; Klümper et al., 2019; Radlinski & Conlon, 2018; Sundberg & Karvonen, 2018), potentially driving the evolution of antibiotic resistance. This may be further shaped by abiotic factors such as presence of antibiotics, which may select for persistence and spread of resistance. These chemicals can also modify the interactions between different infections and, subsequently, the costs of antibiotic resistance (Andersson & Hughes, 2010; Sundberg & Karvonen, 2018). However, most of the studies on effects of bacterial interactions and presence of antibiotics on antimicrobial resistance (AMR) have explored these factors in isolation using bacterial cultures in vitro, therefore largely overlooking the importance of natural heterogeneities and in vivo processes on AMR infections. Thus, studies on costs and benefits of antibiotic resistance in naturally realistic conditions of coinfection and presence of antibiotics are needed.

To gain understanding of the conditions underlying costs of antibiotic resistance, it is essential to capture real-time estimates of key bacterial fitness-related traits: replication, competitive success and virulence (Vaumourin et al., 2015). Here, we conducted in vivo experiments to estimate costs and benefits of antibiotic resistance in pairwise coinfection combinations between antibiotic sensitive strains and resistant mutants of the pathogenic bacterium *Flavobacterium columnare*. We also studied how coinfection with the multicellular parasitic fluke *Diplostomum pseudospathaceum* influenced the fitness-related traits of the bacterium with different profiles of antibiotic resistance. The experiments were performed both in presence and absence of antibiotics to capture the interactions between coinfection and antimicrobials. We used rainbow trout (*Oncorhynchus mykiss*) in the experiments, which is a common natural host for the bacterium and the fluke in aquaculture (Louhi et al., 2015). This makes the system ecologically and economically relevant for exploring the effects of diverse coinfection and antibiotic presence on the cost of antibiotic resistance. We found that the fitness-related traits of antibiotic resistant bacteria were significantly influenced by coinfections and presence of antibiotics. Specific combinations facilitated co-existence of both resistant mutants and sensitive strains and allowed persistence of the resistant bacteria even in absence of antibiotics. Our results exemplify the complexity inherent in determining the costs of antibiotic resistance in naturally occurring interactions.

2 | MATERIALS AND METHODS

2.1 | Preparation of antibiotic resistant bacterial mutants

Two virulent strains of *F. columnare* were used as ancestral strains to generate antibiotic resistant mutants. The broad-spectrum rifampicin was used as a model antibiotic because it effectively selects for resistance mutation in the *rpoB* gene of *F. columnare*. Previously frozen glycerol stocks of *F. columnare* strain B185 (hereafter strain A) and B245 (strain B) were revived from the stocks in 3 mL of modified Shieh medium (Song et al., 1988) on a shaker (200 rpm) at 25°C for 24 h. The optical density (OD, at 570 nm) of the overnight bacterial cultures was measured with spectrophotometer and adjusted to an approximate value of 0.140 (~7.6×10^6 cells mL^{-1}) using the Shieh medium. This minimized differences in the initial density of the strains. Overnight cultures were inoculated into fresh Shieh medium (1:10) and incubated on a shaker (200 rpm) at 25°C for 24 h. The cells were collected by centrifugation (5000 *g*, 5 min, 4°C) and re-suspended in 100 mL of modified Shieh medium. Cells were subsequently spread on modified Shieh plates (100 µL $plate^{-1}$) supplemented with 150 µg mL^{-1} of rifampicin and incubated at room temperature to generate spontaneous resistant mutants (hereafter A^r and B^r, in contrast to sensitive ancestral strains A^s and B^s). After 72 h incubation, single colonies able to grow in 150 µg mL^{-1} rifampicin were inoculated in Shieh medium containing the same rifampicin concentration to confirm resistance of the strains. The stability of the mutation was confirmed by growing the resistant bacteria without rifampicin for 5 days and rechecked for growth in liquid medium. The cultures were stored in 10% glycerol and 10% foetal calf serum at −80°C.

2.2 | Experiment 1: Effect of antibiotic resistance on coinfection between bacterial strains

Real-time abundance and virulence of sensitive ancestral strains and their resistant mutants were assessed in vivo by administering the bacteria to fish hosts in single infection and coinfection combinations. Naïve, uninfected juvenile rainbow trout (*Oncorhynchus mykiss*, average length ± SD = 39.2 ± 3.1 mm) were obtained from a hatchery farm in Central Finland and maintained in aerated groundwater with continuous water flow (17°C) for 2 weeks before the experiments. During the maintenance fish were fed daily with commercial fish food pellets. Prior to the exposures, the water temperature was raised slowly to 25°C (2°C every second day) to meet the optimum growth temperature of *F. columnare* (Ashrafi et al., 2018) and to allow fish acclimation to experimental conditions. A total of 560 fish were divided to 28 treatment groups of 20 fish each and placed individually in small aquaria with 500 mL of groundwater (Table S1; Figure 1).

For single-strain infections, each fish was exposed either to the sensitive strains (A^s, B^s) or resistant mutants (A^r, B^r) using a full-dose (6×10^3 CFU mL^{-1}; 4×20 fish) or a half-dose (3×10^3 CFU mL^{-1}; 4×20 fish) of bacteria. Fish were also co-exposed to the four bacterial strains in all possible pairwise combinations (3×10^3 CFU mL^{-1} of each strain; 6×20 fish) (Table S1; Figure 1). The set-up was also replicated using 10 μg mL^{-1} rifampicin in the exposure water to explore the effect of the presence of antibiotics. Controls receiving pure culture medium, with or without antibiotics, were also included (2×15 fish). Overall, the set-up totalled 610 fish.

The aquaria were randomly placed in a temperature-controlled room and the water temperature was maintained at 25°C throughout the experiment. The fish were monitored for disease symptoms and morbidity for 24 h at 1-h intervals. The experiment was terminated 25 h post-exposure, when all remaining fish were euthanized using terminal anaesthesia (MS-222, Sigma). The fish surviving until the end of the experiment were also euthanized. All fish were measured for total length. To verify *F. columnare* infection from the diseased fish, bacterial cultivations from gills and skin of fish were spread on Shieh agar plates supplemented with tobramycin, which

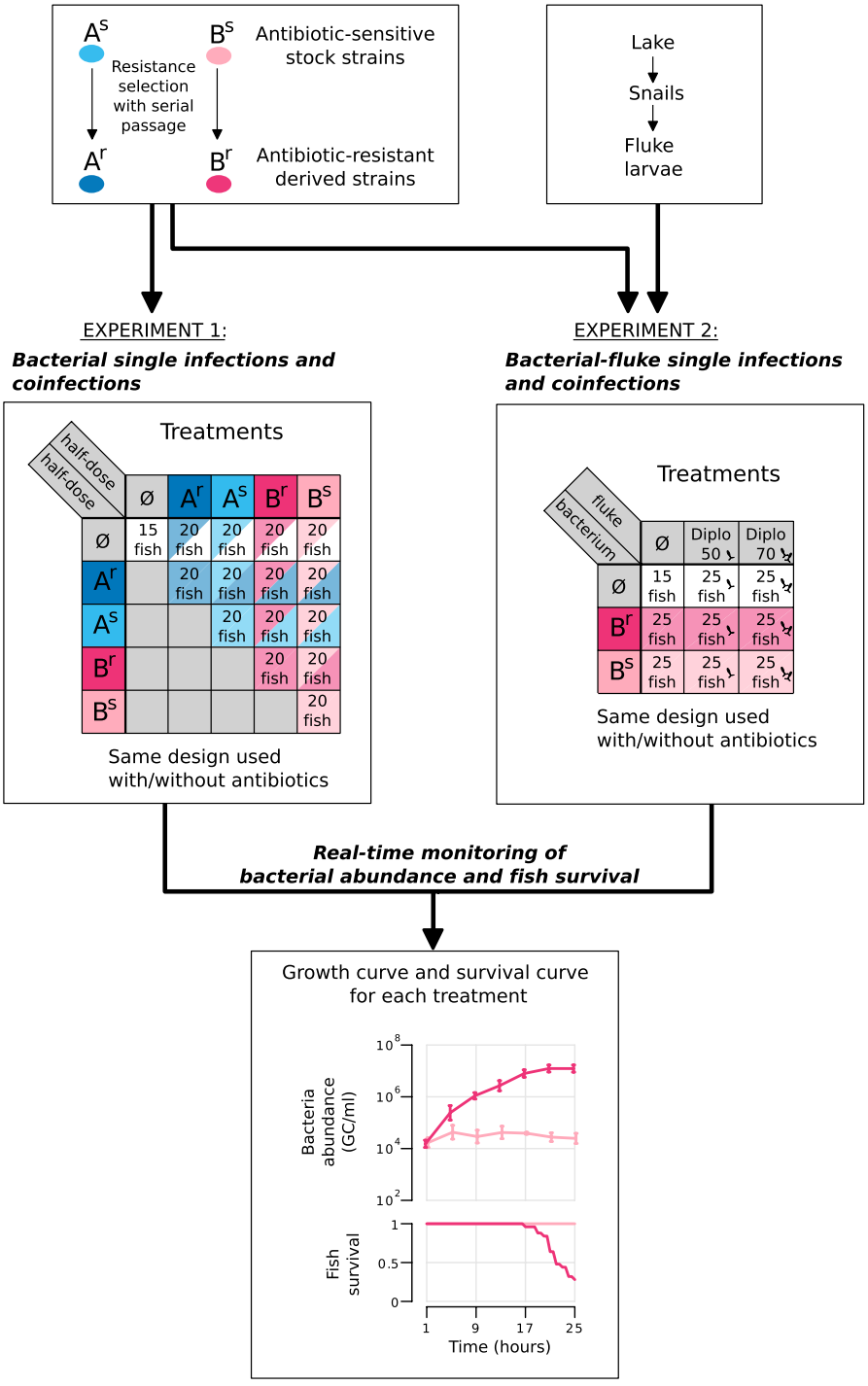

FIGURE 1 Overview of experimental design. In the first phase, antibiotic resistant mutants (A^r, B^r) were produced from ancestral strains (A^s, B^s) through serial passage and used in Experiment 1 (A^s, A^r, B^s, B^r) and Experiment 2 (B^s, B^r). Treatment panels and cells indicate how many fish (rainbow trout, *Oncorhynchus mykiss*) were used in each treatment. In Experiment 1, treatments with two half-doses of the same bacterial strain or mutant correspond to full-dose single infections. In Experiment 2, B^s and B^r correspond to bacterial full-doses, and "Diplo 50" and "Diplo 70" correspond to 50 and 70 cercariae of *Diplostomum pseudospathaceum* administered to each fish. After the exposures, bacterial abundance and fish survival (virulence of infection) were monitored repeatedly up to 25 h. Numbers of flukes successfully infecting the fish were also determined by dissecting the eye lenses.

inhibited growth of other bacteria (Decostere et al., 1997). Yellow colonies with the rhizoid morphology typical for *F. columnare* were considered as a confirmation of infection. Although the experiment was started with two virulent strains, a morphotype change was visually observed in the colonies of the sensitive strain A^s, which is why it turned out to be completely avirulent during the experiment (see also Zhang et al., 2014). Thus, virulence of A^s could not be compared directly to its resistant mutant A^r, or to strain B, in the absence of antibiotics.

2.2.1 | Quantification of bacteria in aquarium water

Bacterial abundance in aquaria water was estimated using qPCR and HRM assays. To quantify bacterial abundance (A^s, B^s, A^r, B^r) in single and coinfection, five aquaria were selected at random from each treatment group at the beginning of the experiment and 100 µL water samples were taken from those aquaria at 1-h post-exposure and every 4 h after that (i.e. at 1, 5, 9, 13, 17, 21 and 25 h). Water samples were treated immediately after sampling with DNase I (final concentration 0.1 mg mL^{-1}) at 37°C for 30 min to degrade extracellular DNA. DNase was then inactivated by adding 0.2 mM EGTA (pH 8.0) and samples were heated at 95°C to break up the cells and to release bacterial DNA. Those DNA samples were then stored at −20°C until qPCR runs. Prior to qPCR runs, DNA samples were thawed and treated with RNase A (final concentration 10 µg mL^{-1}) at 37°C for 30 min to remove RNA. DNA samples were analysed using one or two quantitative methods, depending on the infection treatment.

qPCR using CRISPR regions

A strain-specific qPCR assay based on differences in the bacterial CRISPR (Clustered Regularly Interspaced Short Palindromic Repeats) array was used to measure the abundance of A or B strains in single infections as well as in coinfections between different strains (A^rB^s, A^sB^r, A^sB^s and A^rB^r). Two sets of primers were used to quantify each strain down to a concentration of about 5000 cells mL^{-1} (Table S2). The qPCR assays were performed with 5 µL of DNA samples, 1 µL 300 nM of forward and reverse primers targetting the CRISPR (Clustered Regularly Interspaced Short Palindromic Repeats) regions, 3 µL of water and 10 µL of 2x SYBR Green Supermix (iQ SYBR Green Supermix, Bio-Rad) in a 20 µL reaction volume. All samples were amplified in triplicate. The PCR reaction started at 95°C for 3 min for initial denaturation, followed by 40 cycles of 15 s at 95°C for denaturation, 60 s at 60°C for annealing/extension. A high-resolution melting analysis was performed immediately after amplification to check the quality of the amplified product by increasing the temperature from 55 to 95°C by steps of 0.5°C maintained for 5 s each. Each qPCR run was calibrated using a serial dilution of a stock of purified DNA of the target strain (A or B, depending on the run) for which the DNA concentration had been determined with a Qubit measurement. The serial dilutions comprised seven samples, and the expected final DNA quantities per well for the calibration samples were 2×10^6, 2×10^5, 2×10^4, 2×10^3, 200, 20 and 2 genome copies (GC) per well for strain A, and 1.5×10^6, 1.5×10^5, 1.5×10^4, 1.5×10^3, 150, 15 and 1.5 GC/well for strain B. For each plate, C_q values were calculated using the software provided by the qPCR machine manufacturer (BioRad, CFX Manager Version 3.1.1517.0823). Within each plate, a linear model,

$$C_q = \alpha + \beta \times \log(\text{GC}/\text{well}),$$

was parameterized for α and β using the known GC/well values (number of genome copies per well) and the measured C_q values for all calibration samples. The efficiency of the qPCR reactions was calculated as $-1+10^{(-1/(\beta*\log(10)))}$ and was comprised between 85% and 105% for all plates. For each experimental sample, an estimated number of GC in the sample volume used for qPCR was calculated by averaging the GC/well values from the replicates on the log scale as

$$\text{GC}/\text{well} = \exp\left(\frac{1}{3}\times\sum_{i=1}^{3}\left(\frac{1}{\beta}\left(Cq_i-\alpha\right)\right)\right),$$

where C_{q_1}, C_{q_2}, and C_{q_3} are the C_q values measured for the three replicates of the experimental sample.

qPCR using HRM curves

After identifying diagnostic mutations in the *rpoB* gene by sequencing, a strain-specific high-resolution melting assay (HRM) based on the bacterial *rpoB* gene was developed to determine the proportions of sensitive ancestors and resistant mutants in same-genotype coinfections (treatments A^sA^r and B^sB^r), based on single nucleotide differences in *rpoB* between each mutant and its corresponding ancestral strain. For each strain (A/B), the mutation underlying rifampicin resistance was identified by sequencing eight overlapping fragments encompassing the entire *rpoB* gene (Supplementary methods: "Sequencing *rpoB* gene"). Fragments were amplified using primers based on *rpoB* sequence of *F. columnare* ATCC 49512 (Table S2). Sequence analysis revealed that resistant strains harbour mutations in the *rpoB* gene coding for the β-subunit of the DNA-dependent RNA polymerase (RNAP), which is a molecular target of rifampicin. The mutations were single nucleotide substitutions resulting in amino acid change at codons 491 (C1472A [Ser491Tyr]) and 473 (A1418G [Gln473Arg]) and occurred in A^r and B^r strains, respectively (numbering based on NCBI reference sequence: CP003222.2:2460570–2464382 *Flavobacterium columnare* ATCC 49512 complete genome). Based on homology modelling of the structure of the RNAP β-subunit from *F. columnare* ATCC 49512 using the Phyre2 server (Kelley et al., 2015), those two mutations occur in amino acids located in the rifampicin binding pocket of the protein (comparison with PDB entry 5UAC; Molodtsov et al., 2017). Both the mutations observed in A^r and B^r result in amino acids with larger side chains compared to the sensitive strains, which are likely to substantially affect the interaction between the protein and rifampicin. Importantly, since nucleotide substitutions affect the thermal stability of double-stranded DNA, HRM curves of the amplified

PCR products could be used to estimate the proportions of resistant and sensitive bacteria in water samples from single strain coinfections (B^sB^r and A^sA^r).

PCR amplification was performed in a total volume of 10 μL, containing 5 μL of 2× Precision Melt Supermix (Bio-Rad Laboratories), 1 μL primer mix (forward and reverse, 300 nM) and 4 μL 5 ng μL^{-1} of the DNA template. All samples were amplified in triplicate. The PCR reaction started at 95°C for 1 min for initial denaturation, followed by 40 cycles of 30 s at 95°C for denaturation, 30 s at 63°C for annealing and another 30 s at 72°C for extension. The PCR amplification was then followed by heteroduplex formation by heating at 95°C for 30 s and subsequent cooling at 60°C for 1 min. The high-resolution melting analysis was performed immediately afterwards by increasing the temperature from 65 to 95°C by steps of 0.2°C maintained for 10 s each. Within each plate and for a given strain (A or B), calibration samples prepared by mixing purified DNA from each genotype (sensitive vs. resistant) in known proportions were run. The calibration proportions were 0, 5, 10, 20, 30, 40, 50, 60, 70, 80, 90 and 100% of DNA from the sensitive genotype.

Three measurements were extracted from the normalized relative fluorescence (RF) denaturation curve from each HRM well: the RF value observed at a fixed temperature of 78.6°C, the temperature at which a fixed RF value of 50% was reached, and the melting temperature. A preliminary examination of the relationship between those measurements and the known proportions of sensitive genomes in calibration samples showed that those calibration curves were not monotonic (Figures S1 and S2). To reliably assess genome proportions in experimental samples, B-spline regression was used to fit a within-plate calibration curve for each measurement type (RF at 78.6°C, temperature at 50% RF, and melting temperature). B-splines of degree 3, with one interior knot at proportion = 0.5, were used (a B-spline thus being composed of five basis splines). Their coefficients posteriors were determined using a Bayesian approach and Hamiltonian Monte Carlo sampling as implemented in Stan (Carpenter et al., 2017). We used the rstan package, which provides an interface between R and the Stan program (Stan Development Team, 2020). The model for the observations R_i, T_i, M_i (respectively RF at 78.6°C, temperature at 50% RF, and melting temperature) for the calibration well i with true proportion of sensitive genomes π_i was

$$R_i \sim \text{Normal}\left(\hat{R}_i, \sigma_R\right); \hat{R}_i = \sum_{j=0}^{4} \alpha_j B_j(\pi_i),$$

$$T_i \sim \text{Normal}\left(\hat{T}_i, \sigma_T\right); \hat{T}_i = \sum_{j=0}^{4} \beta_j B_j(\pi_i),$$

$$M_i \sim \text{Normal}\left(\hat{M}_i, \sigma_M\right); \hat{M}_i = \sum_{j=0}^{4} \gamma_j B_j(\pi_i),$$

where $B_{j,0\leqslant j\leqslant 4}$ are the five basis spline functions comprising the B-spline. The priors used were

$$(\sigma_R, \sigma_T, \sigma_M) \sim \text{Normal}(0, 20),$$

$$\alpha_0 \sim \text{Normal}(0.25, 0.5); \alpha_{j,j\geqslant 1} \sim \text{Normal}(0, 1),$$

$$\beta_0 \sim \text{Normal}(78, 4); \beta_{j,j\geqslant 1} \sim \text{Normal}(0, 2),$$

$$\gamma_0 \sim \text{Normal}(78, 4); \gamma_{j,j\geqslant 1} \sim \text{Normal}(0, 2).$$

Once posteriors for the calibration parameters were obtained, they were used to calculate a likelihood profile for the proportion of sensitive genomes in each experimental sample of the same HRM run, based on the three measurements (RF at 78.6°C, temperature at 50% RF and melting temperature) observed for each well of that sample's triplicate and on the same model as above. Assuming a uniform prior for sensitive genome proportions, the proportion posterior was then directly deduced from the likelihood profile and the posterior mean was used as a point estimate of the proportion of sensitive genomes in that experimental sample in downstream analyses. Our method accuracy was assessed by posterior checks where the proportions of sensitive genomes in calibration samples were estimated and compared with the known values (Figures S1 and S2).

2.2.2 | Modelling of bacteria growth curves

Fitting bacterial growth curves

Once detailed counts per strain and genotype were available, bacteria growth data for each of the 40 strain-treatment combinations (4 single infections at full dose, 4 single infections at half-dose, 6 coinfections with 2 strains per coinfection, in the presence and absence of antibiotics ($4+4+6\times2)\times2=40$) were fitted with an equation:

$$\log_{10}(\text{count}(t)) = \alpha + (\beta - \alpha).e^{-kt}.$$

This equation was chosen because it provided a good empirical description of the growth data and had a small number of biologically interpretable parameters: α is the asymptotic value of $\log_{10}(\text{count}(t))$ when $t \to +\infty$, β is the count value at $t=0$, and k is a measure of how fast the growth curve reaches its asymptote (higher k indicating faster growth). The parameters α, β and k were modelled as described below. Note that "trajectory" below means one of the 40 unique combinations of the experimental treatment (determined by (i) antibiotic absence/presence and (ii) identity and size of bacterial inoculums—and when modelling Experiment 2 in a similar way, (iii) *Diplostomum* dose), and the identity of the bacterial strain being counted. For example, the count of A^r bacteria in the treatment "coinfection A^rA^s without antibiotics" was modelled as one trajectory, and the count of A^s bacteria in the same treatment was modelled as another trajectory. The parameters α and k were estimated for each trajectory, and β was estimated for each inoculum size of the counted strain. A random effect of aquarium identity (more precisely, aquarium-by-strain identity, that is for coinfections the effects of aquarium identity on each strain were independent) was added for all growth parameters (α, β and k).

The posterior distributions for each parameter were determined using a Bayesian hierarchical model fitted using the Hamiltonian Monte Carlo approach implemented in Stan (Carpenter et al., 2017)

and the rstan package (Stan Development Team, 2020). The hierarchical model was

$$\hat{y}_{i,t} = \alpha_i + (\beta_i - \alpha_i) \times \exp(-k_i t),$$

$$y_{i,t} \sim \text{StudentT}(\nu, \hat{y}_{i,t}, \sigma_{\text{res}}),$$

where i with $1 \le i \le N_{\text{aquaria-by-strain}}$ is the aquarium-by-strain index, t with $t \in \{1,5,9,13,17,21,25\}$ is the sampling time expressed in hours, $y_{i,t}$ is the observed value of $\log_{10}$(count) for aquarium-strain i at timepoint t and StudentT(ν, $\hat{y}_{i,t}$, σ_{res}) is Student's t-distribution parameterized with degrees of freedom ν, location $\hat{y}_{i,t}$ and scale σ_{res}. This response distribution was chosen to provide some robustness to outliers, especially in the case of counts estimated from HRM-derived proportions. The coefficient values were

$$\alpha_i = \boldsymbol{\alpha}[\text{tr}_i] + \mathbf{re}_{\alpha}[i],$$

$$\beta_i = \boldsymbol{\beta}[\text{ino}_i] + \mathbf{re}_{\beta}[i],$$

$$k_i = \mathbf{k}[\text{tr}_i] + \mathbf{re}_{\mathbf{k}}[i],$$

where i with $1 \le i \le N_{\text{aquaria-by-strain}}$ is still the aquarium-by-strain index, tr_i with $1 \le \text{tr}_i \le N_{\text{trajectories}}$ is the trajectory index for aquarium-strain i, $\boldsymbol{\alpha}$ is a vector of length $N_{\text{trajectories}}$ containing the asymptotic counts for all trajectories, ino_i is the inoculum size index for aquarium-strain i, $\boldsymbol{\beta}$ is a vector of length $N_{\text{inoculumSizes}}$ containing the starting counts for all inoculum sizes, $\mathbf{k}$ is a vector of length $N_{\text{trajectories}}$ containing the growth rates for each trajectory, and $\mathbf{re}_{\alpha}$, $\mathbf{re}_{\beta}$ and $\mathbf{re}_{\mathbf{k}}$ are random effects of the aquarium-by-strain identity such that

$$\mathbf{re}_{\alpha}[i] \sim \text{Normal}(0, \sigma_{\alpha}),$$

$$\mathbf{re}_{\beta}[i] \sim \text{Normal}(0, \sigma_{\beta}),$$

$$\mathbf{re}_{\mathbf{k}}[i] \sim \text{Normal}(0, \sigma_{k}).$$

The priors used for the analysis were

$$\boldsymbol{\alpha}[\text{tr}_i] \sim \text{Normal}(\mu = 5, \sigma = 6) \quad \text{with truncation to } (0, 20),$$

$$\mathbf{k}[\text{tr}_i] \sim \text{Exponential}(\lambda = 1),$$

$$\boldsymbol{\beta}[\text{ino}_i] \sim \text{Normal}(3, 1),$$

$$\sigma_{\alpha} \sim \text{Normal}(0, 0.5),$$

$$\sigma_{k} \sim \text{Normal}(0, 0.05),$$

$$\sigma_{\beta} \sim \text{Normal}(0, 0.5),$$

$$\sigma_{\text{res}} \sim \text{Normal}(0, 0.1),$$

$$(\nu - 1) \sim \text{Exponential}(\lambda = 0.1).$$

Comparison of bacterial abundance at 25 h

Once growth curves had been fitted for each strain-by-treatment combination, posterior distributions of each parameter were available, making it possible to derive the predicted posterior distributions of the bacterial abundance at any time point along the growth trajectories. The posterior distributions for bacterial abundance were calculated at the end of the experiments ($t = 25$ h), individually for each strain-by-treatment combination (Table S3). Bacterial abundances in two treatments were then compared by calculating the posterior of the ratio of the predicted abundances at $t = 25$ h. For example, to compare the abundance of strain A^r in single infection (y_1) with the abundance of strain A^r in mixed infection with A^s (y_2) in the absence of antibiotics, the 95% confidence interval of the posterior distribution of y_1/y_2 was compared with the reference value 1 to determine if y_1 and y_2 were significantly different.

2.2.3 | Survival analysis

Due to the loss of virulence in A^s, full pairwise analysis among the strains on fish survival could not be conducted. Nevertheless, some comparisons of survival in terms of virulence/avirulence of the strains and presence/absence of antibiotics were highlighted. For this purpose, fish survival time was modelled using a Weibull distribution with the survreg function of the survival package in R (Therneau, 2021). The explanatory factors in the survival model were strain type (combinations of strains and inoculum sizes), antibiotic treatment (without/with antibiotics) and their interactions. Fish length was used as a continuous covariate. To avoid fitting issues related to the cases where no death was recorded (e.g. sensitive strains in the presence of antibiotics), the antibiotic variable was centred and coded as −0.5/+0.5 instead of 0/1, so that the reference level for antibiotic was the average between the two antibiotic treatments. For comparison of survival between treatment pairs of interest, marginal means and the corresponding p-values with the reference value of zero were estimated using the emmeans package in R (Russell, 2019).

2.3 | Experiment 2: Effect of antibiotic resistance on coinfection between bacteria and flukes

This experiment used the sensitive and resistant B strain (B^s, B^r), revived and cultured as in Experiment 1. Infected *Lymnaea stagnalis* snails, intermediate hosts of *D. pseudospathaceum* fluke shedding clonal larvae (cercariae), were collected from Lake Vuojärvi (62°24′54″ N, 25°56′14″ E) and stored individually in 1 L of water at 6°C. Before the experiment, eight infected snails were taken to room temperature and allowed to produce cercariae individually in 250 mL of lake water for 3 h. Cercarial suspensions were then combined and cercarial density was estimated from ten subsamples of 1 mL.

Rainbow trout from the same lot as in Experiment 1 were exposed individually to single bacterial strains (6×10^3 CFU mL^{-1}; 2×25 fish), single fluke cercariae using two doses (50 or 70 cercariae/fish; 2×25 fish), or co-exposed simultaneously to both bacterial strains and flukes in four different combinations (4×25 fish). All exposures were also replicated in the presence of antibiotics (10 μg mL^{-1}), totalling to 16 different treatment groups and 400 fish (Table S4; Figure 1). Bacterial treatments without flukes received lake water, and control groups of 30 fish receiving pure culture medium and/or lake water instead of bacteria or flukes, respectively, were also established. Exposures, subsequent monitoring of fish and the sampling for bacterial abundance were done as in the first experiment. The number of *Diplostomum* parasites were counted in the eye lenses of each infected fish at the time of death, except for aquaria/fish used for quantification of bacterial abundance.

2.3.1 | Statistical analysis of Experiment 2

A Bayesian approach was used to fit bacterial growth curves for each treatment and to compare their estimated abundance at 25 h (Table S5) as described for Experiment 1. Analysis of fish survival also followed the same procedure as for Experiment 1, with strain treatment (sensitive/resistant), antibiotic treatment (without/with antibiotics), dose of *Diplostomum* cercariae (three levels, 0/50/70), and their two-way and three-way interactions as explanatory variables. Fish length was used as a covariate. The mean survival times were estimated for each treatment and compared across treatments using the emmeans package in R.

The number of parasites in the eyes of fish was modelled using a generalized linear model (negative binomial distribution with log link function). The explanatory variables were dose of *Diplostomum* (50/70), *F. columnare* strain (sensitive/resistant), the presence of antibiotics (yes/no), and their two-way and three-way interactions. Fish length was used as a covariate. Post-hoc comparisons between treatments of interest were performed using the lsmeans package in R (Lenth, 2016).

3 | RESULTS

3.1 | Experiment 1: Bacterial coinfections in fish host

In this experiment, rainbow trout were challenged with antibiotic sensitive strains (A^s and B^s) and resistant mutants (A^r and B^r) of *F. columnare* in single and coinfection combinations, in presence and absence of antibiotics. Real-time bacterial abundance was measured in vivo using strain-specific qPCR and fish survival was determined over the course of the experiment. In the absence of antibiotics, the abundance of the sensitive strains and the resistant mutants increased over time in both single-infections and coinfection combinations (Figures 2 and 3). Overall abundances in coinfections were lower than the sum of strain abundances in single infections (Table 1), suggesting competitive interactions.

The resistant mutants occupied lower proportion of the bacterial population in all coinfection combinations with the sensitive strains, supporting the idea of cost of resistance as lower competitive ability. However, the proportions of resistant mutants in the coinfections were different depending on whether they were competing with the sensitive strain from the same genotype (A^rA^s and B^rB^s) or from a different genotype (A^rB^s and B^rA^s). The final proportion of A^r was higher when it was coinfecting with B^s compared to coinfection with A^s, and the proportion of B^r during the first half of the experiment (up to 13 h) was higher when coinfecting with A^s compared to coinfection with B^s (Figure 3; Table 2; Figure S3).

The presence of antibiotics changed these dynamics. Similar to single infections (Figure 2), abundances of the coinfecting sensitive strains were effectively reduced by antibiotics (Figure 3), allowing coinfecting resistant mutants to reach higher densities in all combinations (Figure 3; Table S6). Importantly, however, coinfection of sensitive strains with resistant mutants of the same genotype (i.e. A^rA^s and B^rB^s) resulted in most cases in persistence of the sensitive strains regardless of presence of antibiotics, allowing those strains to reach roughly 20–60 times higher densities compared to their corresponding single infections (Figure 3, Table 3).

Survival patterns across different treatments were not analysed because of loss of virulence in A^s. However, it is worth noting that antibiotics decreased virulence in coinfection combinations between B^s and the resistant mutants (i.e. A^rB^s and B^rB^s), but increased it in the combination A^sB^r (Figure 3; Table S7).

3.2 | Experiment 2: Bacteria and fluke co-infections in the fish host

In Experiment 2, rainbow trout were challenged with antibiotic sensitive and resistant *F. columnare* (B^s and B^r) in coinfection with cercariae of the eukaryotic parasitic fluke *D. pseudospathaceum*. Like in Experiment 1, in vivo bacterial abundance and fish survival were determined. Here, the numbers of flukes infecting eyes of fish were also counted. Coinfection with flukes resulted in lower densities of B^s and B^r in the absence of antibiotics, independently of the cercarial dose (Table 4; Figure 4; Figure S4). However, the presence of flukes and the resulting lower bacterial abundance did not change the virulence of infection (Table S8). Importantly, presence of antibiotics removed the negative effect of flukes on abundance of B^r (Figure 4; Table 4) and increased the virulence of the B^r-fluke coinfection compared to B^r single infection (Figure 4; Table S8). Coinfection also influenced the numbers of flukes in eyes of fish depending on the interactions between the bacterial resistance, cercarial dose and presence of antibiotics (Figure S5).

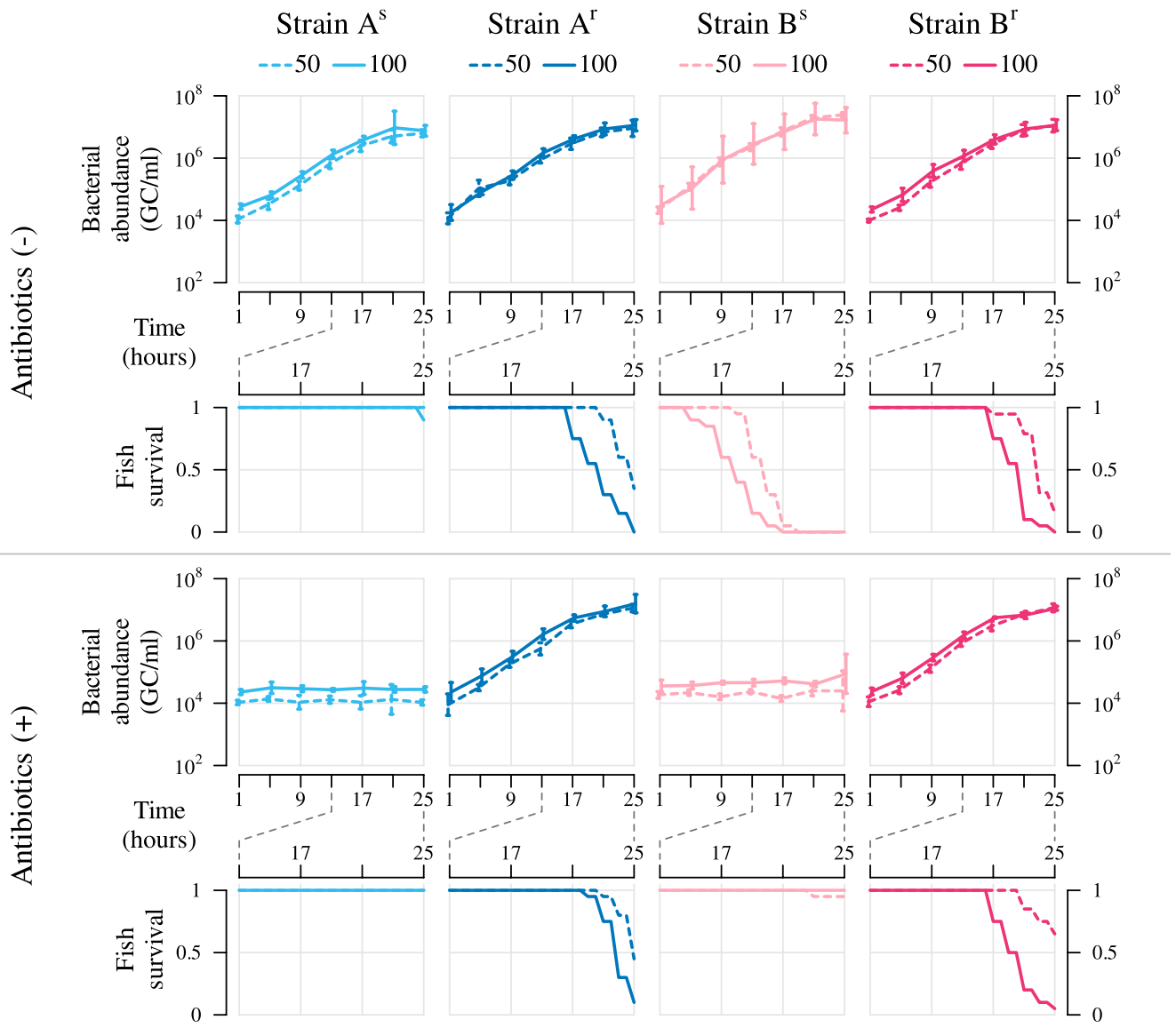

FIGURE 2 Bacterial abundance and survival of host (rainbow trout) as a function of time in single bacterial infections (inoculum sizes 50 or 100) of antibiotic sensitive strains (A^s, B^s) and resistant mutants (A^r, B^r) of *Flavobacterium columnare* in Experiment 1. Bacterial growth curves indicate the estimated mean number of genome copies per mL of aquarium water (GC $mL^{-1} \pm 95\%$ confidence interval) for each time point, calculated from five aquarium replicates. Proportion of fish surviving in each treatment at each time point is estimated from 20 individuals.

4 | DISCUSSION

Challenges of tackling the growing AMR crisis require detailed understanding of the biotic and abiotic factors that influence fitness-related traits of AMR bacteria. This is critical also for the development of management strategies against bacterial diseases. It is important to acknowledge that in nature hosts are typically co-infected with more than one pathogen or parasite species and interactions between the coinfecting partners can directly influence pathogen fitness and disease outcome (Balmer et al., 2009; Hoarau et al., 2020; Susi et al., 2015). Moreover, the external environment, such as the presence of antimicrobials, influences these interactions (Birger et al., 2015; Bottery, Matthews, et al., 2021; Bottery, Pitchford, et al., 2021; Davies et al., 2019; Estrela & Brown, 2018; Klümper et al., 2019). Yet, there is a lack of empirical work combining the effects of coinfections and antimicrobials on fitness-related traits of AMR bacteria infecting their natural hosts in vivo.

Here, we investigated real-time fitness of a pathogenic bacterium in its natural fish host, capturing the effects of bacterial antibiotic resistance, multispecies coinfections and the presence of antibiotics. We found that the costs and benefits of AMR were influenced by the composition of the coinfecting bacterial strains, as well as by the presence of antibiotics, in some cases allowing coexistence of resistant mutants and sensitive strains. Our results also demonstrate that the antibiotic resistant mutants showed lower replication in coinfection with metazoan flukes, while this effect was removed by the presence of antibiotics, resulting in higher virulence of the coinfection. Overall, our results suggest that resistant and sensitive

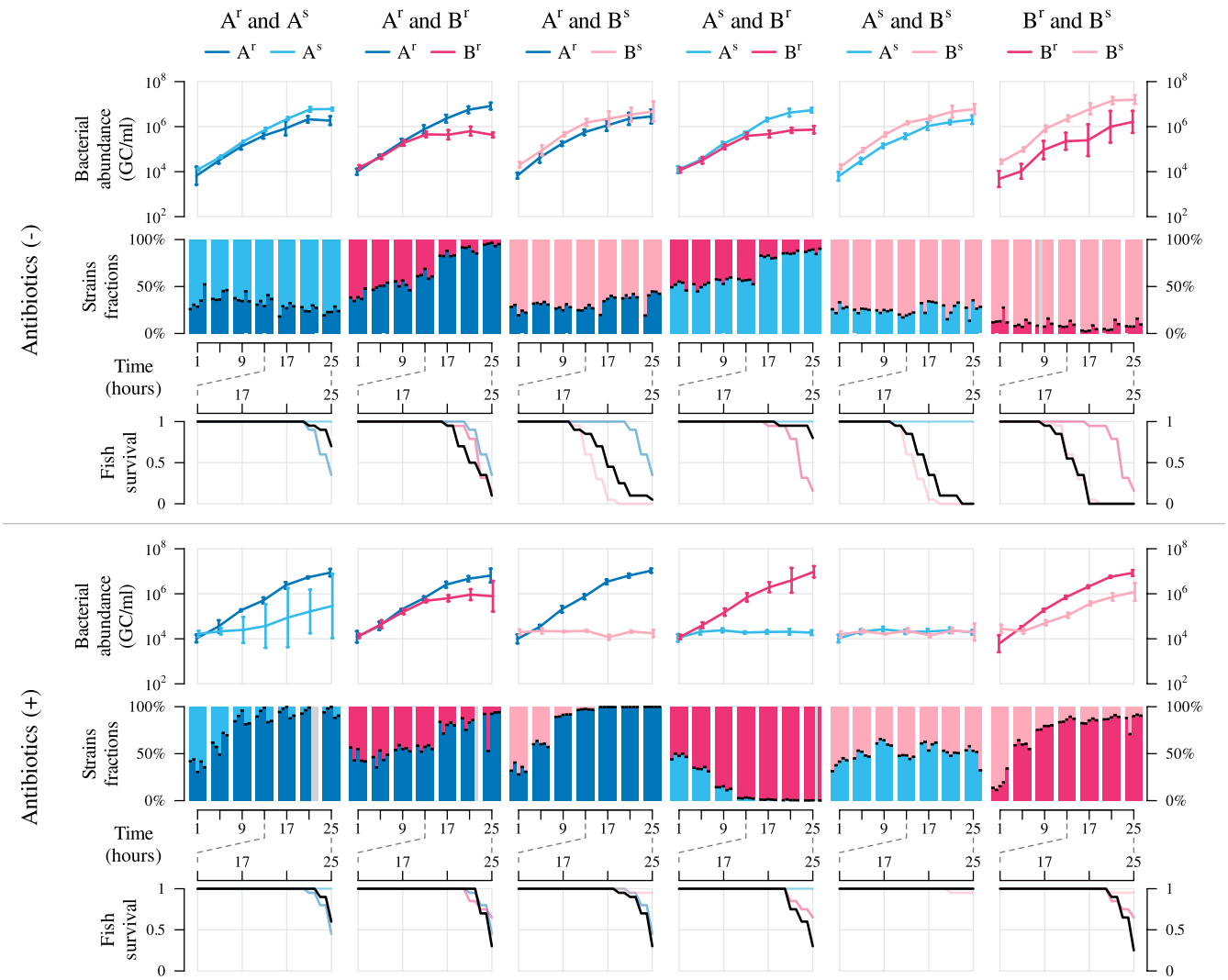

FIGURE 3 Bacterial abundance, strain proportions and survival of host (rainbow trout) as a function of time in coinfection combinations between antibiotic sensitive strains (A^s, B^s) and resistant mutants (A^r, B^r) of *Flavobacterium columnare* in Experiment 1. Bacterial growth curves indicate the estimated mean number of genome copies per mL of aquarium water (GC $mL^{-1} \pm 95\%$ confidence interval) for each time point, calculated from five aquarium replicates. Proportion of fish surviving in each treatment at each time point is estimated from 20 individuals. Survival curves for coinfections are shown in black, with coloured lines added to show the survival curves previously observed for the corresponding single infections (inoculums 50; Figure 1).

bacteria can benefit from coinfection interactions that take place even across different kingdoms. This supports wider implications of the coinfecting community composition for persistence of resistant and sensitive bacterial populations.

Our observation that resistant mutants had lower replication and/or competitive ability in presence of sensitive strains supports the idea of fitness costs of resistance (Melnyk et al., 2015), which is commonly associated with bacterial resistance to the present model antibiotic, rifampicin (Hughes & Brandis, 2013; Melnyk et al., 2015; Song et al., 2014), as well as with chromosomal antibiotic resistance mutations in general (Alekshun & Levy, 2007; Vogwill & MacLean, 2015). Although competitive dominance of sensitive strains in most cases resulted in elimination of resistant mutants in absence of antibiotics, our results demonstrate that the outcome can be influenced by the type of interaction. Resistant mutants were virtually eliminated by the sensitive strains in combinations of the same genotype (A^rA^s and B^rB^s), but when in coinfection with the other genotype (A^rB^s and B^rA^s) they persisted along with the sensitive strain at higher proportions and/or for a longer time. Mechanistically, this result may be caused by dissimilarity of resource requirements in genetically different bacteria (Letten et al., 2021; Song et al., 2014; Wale et al., 2017), or by degree of immunity against bacteriocins produced by the coinfecting strains (Juturu & Wu, 2018). Regardless of the underlying mechanisms, the present results suggest that although competitive exclusion of resistant strains can occur, it may not be an inevitable outcome of competition in absence of antibiotics. These results add to earlier studies on mechanisms promoting persistence of antibiotic resistant and sensitive strains (Borrell et al., 2013; Comas et al., 2011; Estrela & Brown, 2018; Ramadhan & Hegedus, 2005).

TABLE 1 Ratios between the observed total bacterial abundance in coinfections and the expected total abundance of the coinfecting strains based on single infections at $t = 25$ h in absence of antibiotics in Experiment 1.

Observed total abundance of coinfection	Expected total abundance based on single infections	Observed/expected abundance ratio (mean and 95% CI)
A^rA^s	$A^r.50 + A^s.50$	0.55 (0.42–0.71)*
B^rB^s	$B^r.50 + B^s.50$	0.50 (0.39–0.63)*
A^rB^r	$A^r.50 + B^r.50$	0.40 (0.29–0.54)*
A^sB^r	$A^s.50 + B^r.50$	0.32 (0.23–0.43)*
A^rB^s	$A^r.50 + B^s.50$	0.23 (0.18–0.28)*
A^sB^s	$A^s.50 + B^s.50$	0.24 (0.20–0.30)*

Note: The ratios below 1 (i.e. 95% credible intervals not including 1) indicate significantly lower bacterial abundance in coinfection (marked with asterisks). As and Bs, and Ar and Br, refer to antibiotic susceptible strains and resistant mutants, respectively.

TABLE 2 Ratios between the abundance of the coinfecting resistant mutant (A^r, B^r) and total bacterial abundance in coinfection with the sensitive strains (A^s, B^s) at $t = 25$ h in absence of antibiotics in Experiment 1.

Abundance of the resistant mutant in coinfection/Total abundance of coinfection	Ratio (mean and 95% CI)
A^r/A^rA^s	0.25 (0.19–0.32)*
A^r/A^rB^s	0.41 (0.34–0.49)*
B^r/B^rB^s	0.11 (0.07–0.16)*
B^r/B^rA^s	0.11 (0.08–0.14)*

Note: The ratios below 0.5 (i.e. 95% credible intervals not including 0.5) indicate significantly lower abundance of the resistant mutant compared to the sensitive strain (marked with asterisks).

Antibiotics inhibited the growth of sensitive strains. In particular, this pattern was evident in combinations between different genotypes (A^rB^s and B^rA^s) and resulted in increased replication (competitive release) in the resistant mutants. Implications of the clearance of the sensitive strains for the overall virulence of infection, however, depended on the strain identity (A^sB^r resulted in higher virulence and B^sA^r in lower virulence compared to corresponding coinfections in the absence of antibiotics), which may be because of virulence/avirulence or growth differences of the strains. Importantly, our results suggest that antibiotic resistant mutants conferred protection for their ancestral sensitive strains (A^rA^s and B^rB^s) in the presence of antibiotics. This protective effect is interesting since the chromosomal mutations underlying rifampicin resistance should not influence the sensitive strains, for example, through antibiotic-inactivating public goods (Brook, 2004; Perlin et al., 2009) or mutualistic interactions in cross-feeding communities (Adamowicz et al., 2018; Munita & Arias, 2016). Regardless of the detailed mechanisms, the result suggests that sensitive bacteria can survive in presence of antibiotics if facilitated by their coinfecting resistant counterparts. This is interesting also from an applied perspective as it suggests that co-occurring resistant strains in an epidemic could allow sensitive strains, at least partly, to escape antibiotics and grow in presence of treatments, thus potentially accelerating the epidemic. Such

TABLE 3 Ratios between abundance of the sensitive strains (A^s, B^s) or resistant mutants (A^r, B^r) of *F. columnare* in coinfection and their abundance in single infection at $t = 25$ h in presence of antibiotics in Experiment 1.

Coinfection	Single infection	Ratio (mean and 95% CI)
$\mathbf{A^r}A^s$	$A^r.50$	0.68 (0.45–1.00)
$A^r\mathbf{A^s}$	$A^s.50$	22.83 (8.70–49.05)*
$\mathbf{B^r}B^s$	$B^r.50$	0.75 (0.49–1.10)
$B^r\mathbf{B^s}$	$B^s.50$	60.15 (38.14–91.07)*
$\mathbf{A^r}B^r$	$A^r.50$	0.57 (0.38–0.83)*
$A^r\mathbf{B^r}$	$B^r.50$	0.06 (0.04–0.09)*
$\mathbf{A^r}B^s$	$A^r.50$	0.92 (0.61–1.32)
$A^r\mathbf{B^s}$	$B^s.50$	1.00 (0.86–1.16)
$\mathbf{A^s}B^s$	$A^s.50$	1.88 (1.62–2.16)*
$A^s\mathbf{B^s}$	$B^s.50$	0.97 (0.83–1.13)
$\mathbf{A^s}B^r$	$A^s.50$	1.75 (1.50–2.01)*
$A^s\mathbf{B^r}$	$B^r.50$	0.68 (0.44–1.02)

Note: Strains or mutants counted in each coinfection combination are indicated in bold and correspond to those in single 50 dose infections. The ratios above or below 1 (i.e. 95% credible intervals not including 1) indicate significantly higher or lower abundance of the strains or mutants in coinfection (marked with asterisks).

TABLE 4 Ratios between abundance of the sensitive strain (B^s) or of the resistant mutant (B^r) of *F. columnare* in coinfection with *D. pseudospathaceum* fluke (Diplo doses 50 or 70) and their abundance in single infection (bacterial dose 100 in all) or in coinfection with lower Diplo dose in absence or present of antibiotics in Experiment 2.

Coinfection	Single or coinfection	Ratio (mean and 95%CI)
Without antibiotics		
B^r|Diplo.50	B^r	0.55 (0.42–0.71)*
B^r|Diplo.70	B^r	0.52 (0.40–0.66)*
B^r|Diplo.70	B^r|Diplo.50	0.95 (0.72–1.21)
B^s|Diplo.50	B^s	0.77 (0.60–0.98)*
B^s|Diplo.70	B^s	0.62 (0.48–0.78)*
B^s|Diplo.70	B^s|Diplo.50	0.80 (0.63–1.00)
With antibiotics		
B^r|Diplo.50	B^r	0.89 (0.68–1.15)
B^r|Diplo.70	B^r	0.90 (0.69–1.16)
B^r|Diplo.70	B^r|Diplo.50	1.02 (0.77–1.32)
B^s|Diplo.50	B^s	1.00 (0.84–1.18)
B^s|Diplo.70	B^s	1.25 (1.05–1.47)
B^s|Diplo.70	B^s|Diplo.50	1.25 (1.06–1.47)

Note: The ratios below 1 (i.e. 95% credible intervals not including 1) indicate significantly lower abundance of the strains or mutants when in coinfection with flukes (marked with asterisks).

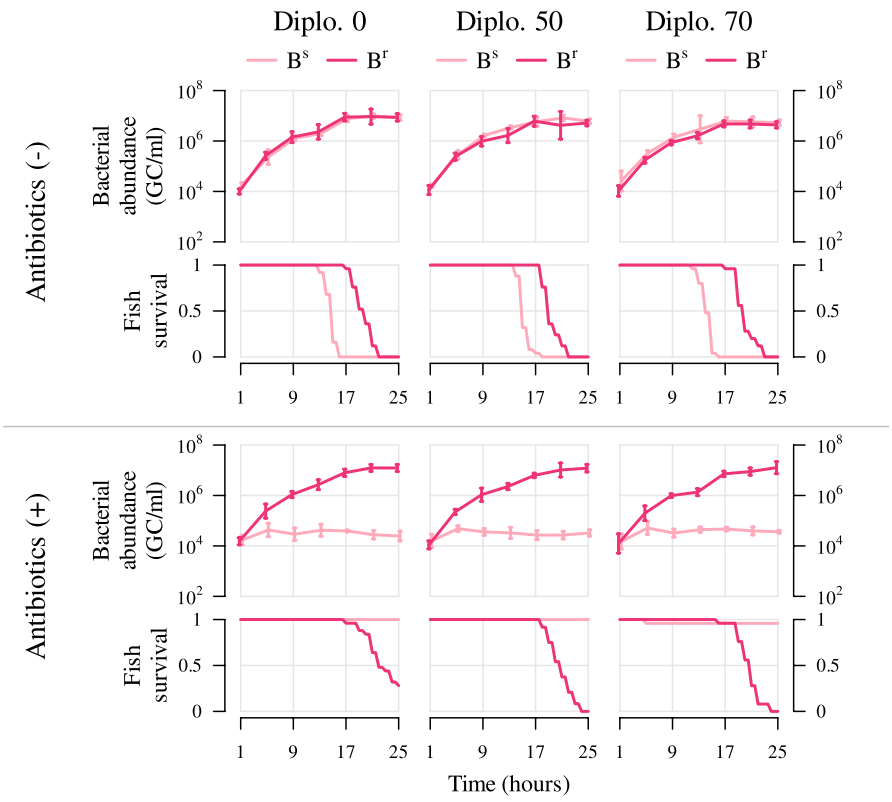

FIGURE 4 Bacterial abundance and host survival in coinfection with the fluke in absence and presence of antibiotics in Experiment 2. Either B^r mutant or B^s strain of *Flavobacterium columnare* was added to the aquaria in single infection (Diplo = 0), or in coinfection with the fluke *Diplostomum pseudospathaceum* (Diplo dose = 50 or 70 cercariae per fish) in the absence or presence of antibiotics. For bacterial growth curves, the estimated number of genome copies per mL of aquarium water (GC mL^{-1}) is shown for each time point as mean value ±95% confidence interval, calculated from five aquarium replicates. Proportion of fish surviving at each time point is calculated from 25 fish per treatment.

conditions could also facilitate emergence of new antibiotic-resistant mutants. Therefore, the combined implications of coinfection interactions and antibiotics may be broader than previously anticipated.

The role of inter-kingdom interactions between pathogens and/or parasites in determining fitness of antibiotic resistant bacteria remains poorly understood (Sundberg & Karvonen, 2018). Here, coinfection with the *Diplostomum* fluke resulted in significantly lower bacterial replication/population size in both resistant and sensitive bacteria, while the overall virulence of infection remained unaltered. Mechanistically, this may be related to direct or indirect host-mediated interactions between the two infections (Louhi et al., 2015). Importantly, the negative effect of the fluke on the replication of the resistant bacteria was removed in presence of antibiotics, resulting in higher overall virulence in coinfection with the parasite. This result suggests that inter-kingdom parasite interactions can have a major impact on fitness-related traits of antibiotic resistant bacteria in presence of antibiotics, providing rare evidence of such interaction in a parasite not targeted by an antibiotic treatment. Thus, antibiotics can benefit resistant bacteria not only by eliminating competing sensitive strains but also by increasing their fitness under coinfection with other parasites. Since both inter-kingdom coinfections and antibiotics are commonly found in different types of environments (Cabello et al., 2013; Karvonen et al., 2019; Read & Taylor, 2001), these findings have broader implications for disease epidemiology and AMR.

In conclusion, we show that interactions between related bacterial strains, as well as inter-kingdom interactions between different parasite taxa, influence the fitness-related traits of sensitive and antibiotic resistant bacteria and thus have the potential to modify evolutionary trajectories of antibiotic resistance. Coinfection, allowing both resistant mutants and sensitive strains to persist in a hostile environment, highlights the fact that responses of multispecies bacterial communities to antibiotic selection can go beyond their performance in isolation. Furthermore, the beneficial effect of antibiotics on replication of the resistant mutants, initially suppressed by another parasite, emphasizes the importance of broad, community-wide interactions between different types of infections. These results are important as increasing use of antibiotics in medicine and food production selects for AMR and results in antibiotic leakage into the environment (Cabello et al., 2013; Klein et al., 2018). Antibiotic residues are particularly common in agriculture and aquaculture (Berendsen et al., 2015; Jansen et al., 2017; Zhang et al., 2016), and bacteria carrying AMR genes are most common in proximity of food production (Wichmann et al., 2014). Because of the antibiotic leakage, residues are detected also in the environment, such as in lakes and rivers, in different concentrations (Kairigo et al., 2020; Kovalakova et al., 2020). Thus, it is clear that antibiotics and AMR influence bacterial dynamics in many different environments. Given this multidimensionality, our results suggest that understanding conditions underlying evolution and spread of antibiotic resistance in natural conditions may be more challenging than previously acknowledged.

AUTHOR CONTRIBUTIONS

R.A., L.-R.S. and A.K. developed the study concept and contributed to experimental design and collected data. R.A. carried out lab work.

V.H. contributed to primer design. M.B. and R.A. analysed and visualized the data. R.A., L.-R.S., M.B., V.H. and A.K. drafted the paper and contributed to editing and revising the paper.

ACKNOWLEDGEMENTS

We thank Kayla King and Ines Klemme for their constructive comments. This work was supported by Academy of Finland (Anssi Karvonen # 310632; Lotta-Riina Sundberg # 314939), OLVI Foundation (Roghaieh Ashrafi#201620393).

CONFLICT OF INTEREST STATEMENT

The authors declare no conflict of interest.

DATA AVAILABILITY STATEMENT

All raw datasets, R scripts and Stan models for statistical analyses are available online from Dryad and Zenodo repositories (https://doi.org/10.5061/dryad.0p2ngf25s).

ORCID

Roghaieh Ashrafi https://orcid.org/0000-0001-8224-5893
Matthieu Bruneaux https://orcid.org/0000-0001-6997-192X

REFERENCES

Adamowicz, E. M., Flynn, J., Hunter, R. C., & Harcombe, W. R. (2018). Cross-feeding modulates antibiotic tolerance in bacterial communities. *The ISME Journal*, *12*(11), 2723–2735. https://doi.org/10.1038/s41396-018-0212-z

Alekshun, M. N., & Levy, S. B. (2007). Molecular mechanisms of antibacterial multidrug resistance. *Cell*, *128*(6), 1037–1050. https://doi.org/10.1016/j.cell.2007.03.004

Alizon, S., de Roode, J. C., & Michalakis, Y. (2013). Multiple infections and the evolution of virulence. *Ecology Letters*, *16*(4), 556–567. https://doi.org/10.1111/ele.12076

Andersson, D. I., & Hughes, D. (2010). Antibiotic resistance and its cost: Is it possible to reverse resistance? *Nature Reviews. Microbiology*, *8*(4), 260–271. https://doi.org/10.1038/nrmicro2319

Ashrafi, R., Bruneaux, M., Sundberg, L. R., Pulkkinen, K., Valkonen, J., & Ketola, T. (2018). Broad thermal tolerance is negatively correlated with virulence in an opportunistic bacterial pathogen. *Evolutionary Applications*, *11*(9), 1700–1714. https://doi.org/10.1111/eva.12673

Balmer, O., Stearns, S. C., Schötzau, A., & Brun, R. (2009). Intraspecific competition between co-infecting parasite strains enhances host survival in African trypanosomes. *Ecology*, *90*(12), 3367–3378. https://doi.org/10.1890/08-2291.1

Berendsen, B. J. A., Wegh, R. S., Memelink, J., Zuidema, T., & Stolker, L. A. M. (2015). The analysis of animal faeces as a tool to monitor antibiotic usage. *Talanta*, *132*, 258–268. https://doi.org/10.1016/j.talanta.2014.09.022

Birger, R. B., Kouyos, R. D., Cohen, T., Griffiths, E. C., Huijben, S., Mina, M. J., Volkova, V., Grenfell, B., & Metcalf, C. J. E. (2015). The potential impact of coinfection on antimicrobial chemotherapy and drug resistance. *Trends in Microbiology*, *23*(9), 537–544. https://doi.org/10.1016/j.tim.2015.05.002

Borrell, S., Teo, Y., Giardina, F., Streicher, E. M., Klopper, M., Feldmann, J., Müller, B., Victor, T. C., & Gagneux, S. (2013). Epistasis between antibiotic resistance mutations drives the evolution of extensively drug-resistant tuberculosis. *Evolution, Medicine, and Public Health*, *2013*(1), 65–74. https://doi.org/10.1093/emph/eot003

Bottery, M. J., Matthews, J. L., Wood, A. J., Johansen, H. K., Pitchford, J. W., & Friman, V.-P. (2021). Inter-species interactions alter antibiotic efficacy in bacterial communities. *The ISME Journal*, *16*, 812–821. https://doi.org/10.1038/s41396-021-01130-6

Bottery, M. J., Pitchford, J. W., & Friman, V.-P. (2021). Ecology and evolution of antimicrobial resistance in bacterial communities. *The ISME Journal*, *15*(4), 939–948. https://doi.org/10.1038/s41396-020-00832-7

Briaud, P., Camus, L., Bastien, S., Doléans-Jordheim, A., Vandenesch, F., & Moreau, K. (2019). Coexistence with *Pseudomonas aeruginosa* alters *Staphylococcus aureus* transcriptome, antibiotic resistance and internalization into epithelial cells. *Scientific Reports*, *9*(1), 16564. https://doi.org/10.1038/s41598-019-52975-z

Brook, I. (2004). β-Lactamase-producing bacteria in mixed infections. *Clinical Microbiology and Infection*, *10*(9), 777–784.

Cabello, F. C., Godfrey, H. P., Tomova, A., Ivanova, L., Dölz, H., Millanao, A., & Buschmann, A. H. (2013). Antimicrobial use in aquaculture re-examined: Its relevance to antimicrobial resistance and to animal and human health. *Environmental Microbiology*, *15*(7), 1917–1942. https://doi.org/10.1111/1462-2920.12134

Carpenter, B., Gelman, A., Hoffman, M. D., Lee, D., Goodrich, B., Betancourt, M., Brubaker, M. A., Guo, J., Li, P., & Riddell, A. (2017). Stan: A probabilistic programming language. *Journal of Statistical Software*, *76*(1), 1–32. https://doi.org/10.18637/jss.v076.i01

Comas, I., Borrell, S., Roetzer, A., Rose, G., Malla, B., Kato-Maeda, M., Galagan, J., Niemann, S., & Gagneux, S. (2011). Whole-genome sequencing of rifampicin-resistant *Mycobacterium tuberculosis* strains identifies compensatory mutations in RNA polymerase genes. *Nature Genetics*, *44*(1), 106–110. https://doi.org/10.1038/ng.1038

Davies, N. G., Flasche, S., Jit, M., & Atkins, K. E. (2019). Within-host dynamics shape antibiotic resistance in commensal bacteria. *Nature Ecology & Evolution*, *3*(3), 440–449. https://doi.org/10.1038/s41559-018-0786-x

de Roode, J. C., Culleton, R., Bell, A. S., & Read, A. F. (2004). Competitive release of drug resistance following drug treatment of mixed *Plasmodium chabaudi* infections. *Malaria Journal*, *3*, 33. https://doi.org/10.1186/1475-2875-3-33

de Roode, J. C., Pansini, R., Cheesman, S. J., Helinski, M. E. H., Huijben, S., Wargo, A. R., Bell, A. S., Chan, B. H., Walliker, D., & Read, A. F. (2005). Virulence and competitive ability in genetically diverse malaria infections. *Proceedings of the National Academy of Sciences of the United States of America*, *102*(21), 7624–7628. https://doi.org/10.1073/pnas.0500078102

Decostere, A., Haesebrouck, F., & Devriese, L. A. (1997). Shieh medium supplemented with tobramycin for selective isolation of *Flavobacterium columnare* (*Flexibacter columnaris*) from diseased fish. *Journal of Clinical Microbiology*, *35*(1), 322–324. https://doi.org/10.1128/jcm.35.1.322-324.1997

Estrela, S., & Brown, S. P. (2018). Community interactions and spatial structure shape selection on antibiotic resistant lineages. *PLoS Computational Biology*, *14*(6), e1006179. https://doi.org/10.1371/journal.pcbi.1006179

Hall, B. G. (2004). Predicting the evolution of antibiotic resistance genes. *Nature Reviews. Microbiology*, *2*(5), 430–435. https://doi.org/10.1038/nrmicro888

Hiltunen, T., Virta, M., & Laine, A.-L. (2017). Antibiotic resistance in the wild: An eco-evolutionary perspective. *Philosophical Transactions of the Royal Society of London. Series B, Biological Sciences*, *372*(1712), 20160039. https://doi.org/10.1098/rstb.2016.0039

Hoarau, A. O. G., Mavingui, P., & Lebarbenchon, C. (2020). Coinfections in wildlife: Focus on a neglected aspect of infectious disease epidemiology. *PLoS Pathogens*, *16*(9), e1008790. https://doi.org/10.1371/journal.ppat.1008790

Hughes, D., & Brandis, G. (2013). Rifampicin resistance: Fitness costs and the significance of compensatory evolution. *Antibiotics*, *2*(2), 206–216.

Jansen, L. J., Bolck, Y. J., Rademaker, J., Zuidema, T., & Berendsen, B. J. (2017). The analysis of tetracyclines, quinolones, macrolides, lincosamides, pleuromutilins, and sulfonamides in chicken feathers using UHPLC-MS/MS in order to monitor antibiotic use in the poultry sector. *Analytical and Bioanalytical Chemistry*, *409*(21), 4927–4941.

Johnson, P. T. J., de Roode, J. C., & Fenton, A. (2015). Why infectious disease research needs community ecology. *Science*, *349*(6252), 1259504. https://doi.org/10.1126/science.1259504

Juturu, V., & Wu, J. C. (2018). Microbial production of bacteriocins: Latest research development and applications. *Biotechnology Advances*, *36*(8), 2187–2200. https://doi.org/10.1016/j.biotechadv.2018.10.007

Kairigo, P., Ngumba, E., Sundberg, L.-R., Gachanja, A., & Tuhkanen, T. (2020). Occurrence of antibiotics and risk of antibiotic resistance evolution in selected Kenyan wastewaters, surface waters and sediments. *The Science of the Total Environment*, *720*, 137580. https://doi.org/10.1016/j.scitotenv.2020.137580

Karvonen, A., Jokela, J., & Laine, A. L. (2019). Importance of sequence and timing in parasite coinfections. *Trends in Parasitology*, *35*(2), 109–118.

Kelley, L. A., Mezulis, S., Yates, C. M., Wass, M. N., & Sternberg, M. J. (2015). The Phyre2 web portal for protein modeling, prediction and analysis. *Nature Protocols*, *10*(6), 845–858.

Klein, E. Y., van Boeckel, T., Martinez, E. M., Pant, S., Gandra, S., Levin, S. A., Goossens, H., & Laxminarayan, R. (2018). Global increase and geographic convergence in antibiotic consumption between 2000 and 2015. *Proceedings of the National Academy of Sciences of the United States of America*, *115*(15), E3463–E3470. https://doi.org/10.1073/pnas.1717295115

Klümper, U., Recker, M., Zhang, L., Yin, X., Zhang, T., Buckling, A., & Gaze, W. H. (2019). Selection for antimicrobial resistance is reduced when embedded in a natural microbial community. *The ISME Journal*, *13*(12), 2927–2937. https://doi.org/10.1038/s41396-019-0483-z

Kovalakova, P., Cizmas, L., McDonald, T. J., Marsalek, B., Feng, M., & Sharma, V. K. (2020). Occurrence and toxicity of antibiotics in the aquatic environment: A review. *Chemosphere*, *251*, 126351. https://doi.org/10.1016/j.chemosphere.2020.126351

Lenth, R. V. (2016). Least-squares means: The *R* package lsmeans. *Journal of Statistical Software*, *69*(1), 1–33. https://doi.org/10.18637/jss.v069.i01

Letten, A. D., Hall, A. R., & Levine, J. M. (2021). Using ecological coexistence theory to understand antibiotic resistance and microbial competition. *Nature Ecology & Evolution*, *5*(4), 431–441. https://doi.org/10.1038/s41559-020-01385-w

Louhi, K.-R., Sundberg, L.-R., Jokela, J., & Karvonen, A. (2015). Interactions among bacterial strains and fluke genotypes shape virulence of co-infection. *Proceedings of the Royal Society B: Biological Sciences*, *282*(1821), 20152097.

Melnyk, A. H., Wong, A., & Kassen, R. (2015). The fitness costs of antibiotic resistance mutations. *Evolutionary Applications*, *8*(3), 273–283. https://doi.org/10.1111/eva.12196

Molodtsov, V., Scharf, N. T., Stefan, M. A., Garcia, G. A., & Murakami, K. S. (2017). Structural basis for rifamycin resistance of bacterial RNA polymerase by the three most clinically important *RpoB* mutations found in *Mycobacterium tuberculosis*. *Molecular Microbiology*, *103*(6), 1034–1045.

Munita, J. M., & Arias, C. A. (2016). Mechanisms of antibiotic resistance. In I. T. Kudva, N. A. Cornick, P. J. Plummer, Q. Zhang, T. L. Nicholson, J. P. Bannantine, & B. H. Bellaire (Eds.), *Virulence mechanisms of bacterial pathogens* (pp. 481–511). ASM Press. https://doi.org/10.1128/9781555819286.ch17

Pedersen, A. B., & Fenton, A. (2019). Wild rodents as a natural model to study within-host parasite interactions. In K. Wilson, A. Fenton, & D. Tompkins (Eds.), *Wildlife disease ecology: Linking theory to data and application* (pp. 58–90). Cambridge University Press. https://doi.org/10.1017/9781316479964.003

Perlin, M. H., Clark, D. R., McKenzie, C., Patel, H., Jackson, N., Kormanik, C., Powell, C., Bajorek, A., Myers, D. A., Dugatkin, L. A., & Atlas, R. M. (2009). Protection of *Salmonella* by ampicillin-resistant *Escherichia coli* in the presence of otherwise lethal drug concentrations. *Proceedings of the Royal Society of London Series B, Biological sciences*, *276*(1674), 3759–3768. https://doi.org/10.1098/rspb.2009.0997

Radlinski, L., & Conlon, B. P. (2018). Antibiotic efficacy in the complex infection environment. *Current Opinion in Microbiology*, *42*, 19–24. https://doi.org/10.1016/j.mib.2017.09.007

Ramadhan, A. A., & Hegedus, E. (2005). Survivability of vancomycin resistant enterococci and fitness cost of vancomycin resistance acquisition. *Journal of Clinical Pathology*, *58*(7), 744–746. https://doi.org/10.1136/jcp.2004.024091

Read, A. F., & Taylor, L. H. (2001). The ecology of genetically diverse infections. *Science*, *292*(5519), 1099–1102. https://doi.org/10.1126/science.1059410

Rowan-Nash, A. D., Korry, B. J., Mylonakis, E., & Belenky, P. (2019). Cross-domain and viral interactions in the microbiome. *Microbiology and Molecular Biology Reviews: MMBR*, *83*(1), e00044-18. https://doi.org/10.1128/MMBR.00044-18

Russell, L. (2019). *Emmeans: Estimated marginal means, aka least-squares means*. R Package Version 1.4.2. https://sciwheel.com/work/citation?ids=12861174&pre=&suf=&sa=0&dbf=0

Seppälä, O., Karvonen, A., Rellstab, C., Louhi, K.-R., & Jokela, J. (2012). Reciprocal interaction matrix reveals complex genetic and dose-dependent specificity among coinfecting parasites. *The American Naturalist*, *180*(3), 306–315. https://doi.org/10.1086/666985

Song, T., Park, Y., Shamputa, I. C., Seo, S., Lee, S. Y., Jeon, H., Choi, H., Lee, M., Glynne, R. J., Barnes, S. W., Walker, J. R., Batalov, S., Yusim, K., Feng, S., Tung, C. S., Theiler, J., Via, L. E., Boshoff, H. I., Murakami, K. S., … Cho, S. N. (2014). Fitness costs of rifampicin resistance in *Mycobacterium tuberculosis* are amplified under conditions of nutrient starvation and compensated by mutation in the β' subunit of RNA polymerase. *Molecular Microbiology*, *91*(6), 1106–1119.

Song, Y. L., Fryer, J. L., & Rohovec, J. S. (1988). Comparison of six media for the cultivation of *Flexibacter columnaris*. *Fish Pathology*, *23*(2), 91–94. https://doi.org/10.3147/jsfp.23.91

Stan Development Team. (2020). *RStan: The R interface to Stan*. R Package Version 2.21.2. https://mc-stan.org/

Sundberg, L.-R., & Karvonen, A. (2018). Minor environmental concentrations of antibiotics can modify bacterial virulence in co-infection with a non-targeted parasite. *Biology Letters*, *14*(12), 20180663. https://doi.org/10.1098/rsbl.2018.0663

Susi, H., Barrès, B., Vale, P. F., & Laine, A.-L. (2015). Co-infection alters population dynamics of infectious disease. *Nature Communications*, *6*, 5975. https://doi.org/10.1038/ncomms6975

Therneau, T. (2021). *A package for survival analysis in R*. Rpackage Version 3.2-10.2021. https://sciwheel.com/work/citation?ids=12861142&pre=&suf=&sa=0&dbf=0

Vaumourin, E., Vourc'h, G., Gasqui, P., & Vayssier-Taussat, M. (2015). The importance of multiparasitism: Examining the consequences of co-infections for human and animal health. *Parasites & Vectors*, *8*, 545. https://doi.org/10.1186/s13071-015-1167-9

Vogwill, T., & MacLean, R. C. (2015). The genetic basis of the fitness costs of antimicrobial resistance: A meta-analysis approach. *Evolutionary Applications*, *8*(3), 284–295. https://doi.org/10.1111/eva.12202

Wale, N., Sim, D. G., Jones, M. J., Salathe, R., Day, T., & Read, A. F. (2017). Resource limitation prevents the emergence of drug resistance by intensifying within-host competition. *Proceedings of the National Academy of Sciences of the United States of America*, *114*(52), 13774–13779. https://doi.org/10.1073/pnas.1715874115

Wargo, A. R., Huijben, S., de Roode, J. C., Shepherd, J., & Read, A. F. (2007). Competitive release and facilitation of drug-resistant parasites after therapeutic chemotherapy in a rodent malaria model. *Proceedings of the National Academy of Sciences of the United States of America*, *104*(50), 19914–19919. https://doi.org/10.1073/pnas.0707766104

Wichmann, F., Udikovic-Kolic, N., Andrew, S., & Handelsman, J. (2014). Diverse antibiotic resistance genes in dairy cow manure. *mBio*, *5*, e01017-13.

World Health Organization. (2018). *WHO report on surveillance of antibiotic consumption: 2016–2018 early implementation*.

Zhang, J., Laakso, J., Mappes, J., Laanto, E., Ketola, T., Bamford, J. K. H., Kunttu, H., & Sundberg, L.-R. (2014). Association of colony morphotypes with virulence, growth and resistance against protozoan predation in the fish pathogen *Flavobacterium columnare*. *FEMS Microbiology Ecology*, *89*(3), 553–562. https://doi.org/10.1111/1574-6941.12356

Zhang, Z., Li, X., Ding, S., Jiang, H., Shen, J., & Xia, X. (2016). Multiresidue analysis of sulfonamides, quinolones, and tetracyclines in animal tissues by ultra-high performance liquid chromatography-tandem mass spectrometry. *Food Chemistry*, *204*, 252–262. https://doi.org/10.1016/j.foodchem.2016.02.142

SUPPORTING INFORMATION

Additional supporting information can be found online in the Supporting Information section at the end of this article.

How to cite this article: Ashrafi, R., Bruneaux, M., Sundberg, L.-R., Hoikkala, V., & Karvonen, A. (2023). Multispecies coinfections and presence of antibiotics shape resistance and fitness costs in a pathogenic bacterium. *Molecular Ecology*, *00*, 1–14. https://doi.org/10.1111/mec.17040